ADVANCED MATERIALS
www.advmat.de

www.MaterialsViews.com

Spray-Processable Blue-to-Highly Transmissive Switching Polymer Electrochromes via the Donor–Acceptor Approach

By *Chad M. Amb, Pierre M. Beaujuge,* and *John R. Reynolds**

Relying on low-power stimulated optical changes, non-emissive electrochromic (EC) technologies can be operated under a wide range of viewing angles and lighting conditions (e.g., direct sunlight), making them especially desirable in the development of flexible-display-device applications including electronic papers (e-papers) and large-area information panels.[1,2] With their applicability in scalable and cost-effective manufacturing processes spanning inkjet- and flexo-printing, solution-processable π-conjugated polymers are finding the path to commercialization in several areas including solar power conversion[3] and are now expected to be applied to various transmissive/reflective electrochromic device (ECD) configurations.[1] However, for electrochromic polymers (ECPs) to compete with the more established electrophoretic technologies, their potential for color tunability should be confirmed by extending the design and synthesis of polymer electrochromes to a palette of derivatives possessing complementary color states, as well as a redox accessible transmissive state.

The homopolymerization of dioxythiophenes[4–7] (DOTs) and other electron-rich monomers[8–10] with a high-lying highest occupied molecular orbital (HOMO) commonly produces narrow-bandgap materials absorbing in the red region of the visible spectrum, hence, exhibiting colors ranging from purple to dark blue. Nonetheless, it is worth noting that only a few are, at the same time, solution-processable (the vast majority being electropolymerized from unsubstituted monomers), cathodically coloring, and fast-switching analogues with long-term stability on repeated electrochemical switching.[8,11] In parallel, the "donor–acceptor" (DA) approach,[12] now frequently applied to macromolecular systems in the context of bandgap engineering, has recently been employed to achieve blue-to-clear switching ECPs incorporating low-lying lowest unoccupied molecular orbital (LUMO) moieties such as cyanovinylene[13] and benzotriazole,[14] thus, introducing the perspective of reducing the electron-rich character of the backbone, while retaining the low bandgap producing the desired blue color. In spite of these developments, designing neutral-state blue polymer electrochromes combining solution processability, high contrast ratios attainable in subsecond switching times, and long-term redox stability (over 10000 cycles) represents the next logical step towards truly useful EC materials.

In recent work, we investigated the effect of varying the relative contribution of electron-rich and electron-deficient heterocycles composing the polymer repeat unit on the absorption spectrum of a series of well-defined π-conjugated polymers containing various DOTs and 2,1,3-benzothiadiazole (BTD) as the accepting component (see Fig. 1a **P1**–**P3**).[15] These polymers were shown to possess a dual band of absorption in the visible spectrum consisting of a short- and a long-wavelength absorption band, which can be modulated in terms of their relative intensity, wavelength maxima, and absorption onsets as a function of the DA content in the main-chain. In particular, when the local minimum of absorption separating these two optical transitions was positioned in the 500–550-nm range, the resulting ECPs were found to exhibit the color green,[16] a color-state historically difficult to achieve in the field of π-conjugated polymers.[17,18]

Herein, we demonstrate how the dual band of absorption found in macromolecular π-conjugated systems alternating electron-rich and -poor heterocycles[15,19–22] can be tailored to open a broad window of transmission in the high-energy region of the visible spectrum, with the goal of producing neutral-state saturated blue ECPs. In this instance, the extent of electron-rich building units along the polymer backbone has been reduced to a point where the short-wavelength absorption band of the polymer is fully transferred into the UV to maximize the blue transmission, while the long-wavelength optical transition extends from the green region up to the near-IR (see Fig. 1b, **P4a**). Our approach is exemplified by a series of spray-processable cathodically coloring polymer electrochromes that switch to a highly transmissive oxidized state on electrochemical doping. The corresponding polymers are linear, strictly alternating in terms of their DA content (see Fig. 1c **P4a**–**P4c**), and possess oxidation potentials sufficiently high to provide ambient stability [in contrast with the majority of their all-donor counterparts including poly(3,4-ethylenedioxythiophene) (PEDOT)][7] but low enough to allow fast and reversible redox switching on repeated cycling. In addition, an ester-functionalized DA electrochrome (**P4c**) was achieved by solubilizing side chains that can be chemically removed in a postdeposition processing step to produce films insoluble in conventional organic solvents that retain their electroactivity. Our strategy offers perspectives for the fabrication of long-lived electrolyte-based switchable devices, as well as in the processing of vertically stacked ECDs with multiple electroactive layers.

[*] Prof. J. R. Reynolds, Dr. C. M. Amb, Dr. P. M. Beaujuge
The George and Josephine Butler Polymer Research Laboratory
Department of Chemistry
Center for Macromolecular Science and Engineering
University of Florida
Gainesville, FL, 32611 (USA)
E-mail: reynolds@chem.ufl.edu

DOI: 10.1002/adma.200902917

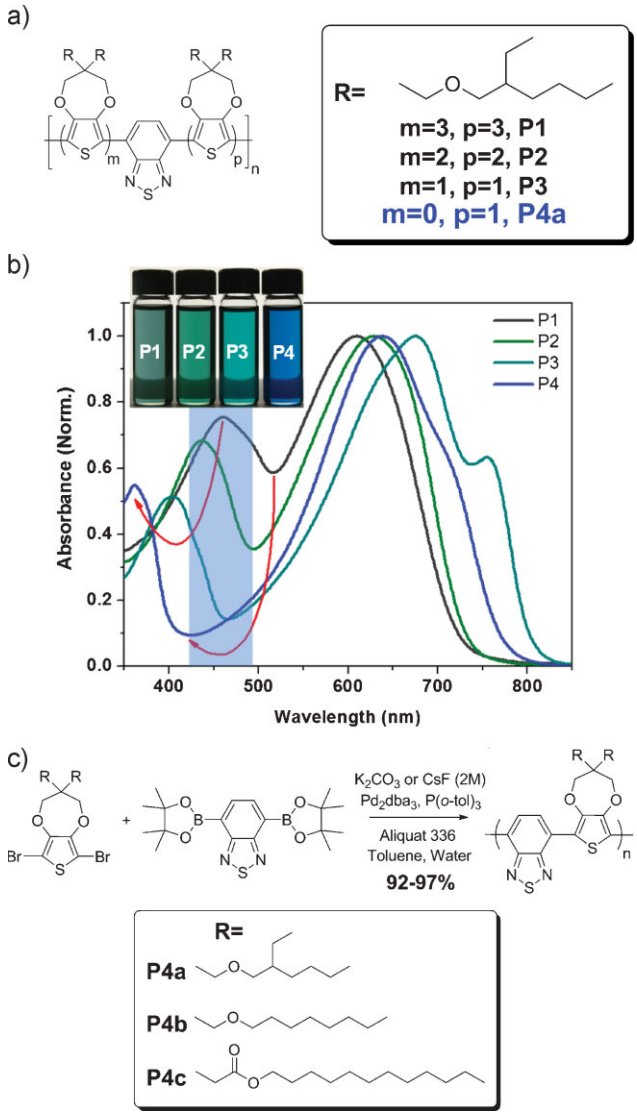

Figure 1. a) Structures of DA copolymers **P1**–**P4a** differing by the number of electron-rich and -poor heterocycles incorporated in the repeat unit. b) UV–vis solution absorption spectra of **P1**–**P4a** in toluene (the spectra are normalized at the longer-wavelength absorption maximum of the polymers). The inset shows the various colors obtained across the polymer series as a function of the DA ratio constitutive of the repeat unit. c) **P4a**–**P4c** are polymerized by inverting the monomer functionalities in comparison with conventional Pd-mediated Suzuki cross-coupling methodologies employed.

While the origin of the dual-band absorption sometimes encountered in DA-type semiconducting polymers remains a source of debate, two mainstream rationales have been frequently proposed. A first assumption attributes the lower-energy optical transition to the presence of intramolecular charge-transfer excitons occurring on the presence of covalently bound DA segments along the backbone.[23,24] A second assumption considers the presence of low-lying unoccupied energy levels, strictly localized on the electron-deficient heterocycles, yet forming a discrete "band" of easily accessed energy states within the "bandgap" of the conjugated system in its ground state.[16,25–27] In both cases, the higher-energy transitions appear localized on the most-electron-rich building units incorporated along the polymer backbone with a clear dependence on their relative concentration to the electron-deficient heterocycles.[15] This distinct contribution from the electron-rich segments on the short-wavelength absorption band in DA backbones is illustrated in Figure 1b, where the said optical transition undergoes a hypsochromic shift ranging from 25 to 40 nm as the number of 3,4-propylenedioxythiophene (ProDOT) units incorporated in the repeat unit is decreased from 6 (**P1**), to 4 (**P2**), and to 2 (**P3**) units. In parallel, the long-wavelength absorption band red shifts with increasing number of BTDs in the repeat unit, and the peak-to-peak distance between the two bands of absorption increases dramatically, hence, opening a window of transmission in the blue-green region of the visible.

With the idea of extending this window of transmission into the blue region of the spectrum by fully rejecting the high-energy optical transition into the UV, the synthesis of a strictly alternating DA copolymer of ProDOT and BTD was envisioned (see Fig. 1a, **P4a**). In contrast with **P1**–**P3**, which were chemically polymerized from symmetrical donor–acceptor–donor (DAD) oligomers via the mild oxidizing agent $FeCl_3$,[15] a palladium-mediated polycondensation route had to be introduced to afford the desired DA alternating pattern. However, the relative difficulty and particularly low yields associated with the synthesis of difunctionalized organostannane and organoborane derivatives of dioxythiophenes prevented us from using common polymerization methodology, whereby the most electron-poor heterocycle acts as the "electrophile" (which undergoes oxidative addition) and the electron-rich counterpart acts as the "nucleophile" (in transmetallation).[20,28–31] Scanning the literature, we found a unique example of a DA copolymer synthesized by inverting the functionalities between donor and acceptor.[32,33] In this work, BTD was difunctionalized with pinacol ester-protected boronic acid in a one-step Miyaura borylation. Upon optimization of the step relative to the synthesis of the organoborane derivative of BTD (see Experimental section), two dialkoxy-substituted ProDOT–BTD copolymers (namely **P4a** and **P4b**) were subsequently produced in excellent yields (>90%), with number average molecular weights (M_n) as high as 23 kDa by using traditional Suzuki cross-coupling conditions (see Fig. 1c). In addition, a didodecylester-substituted DA analogue, namely **P4c**, was successfully achieved ($M_n = 11.1$ kDa) using a modification of the base-free Suzuki conditions described earlier by our group.[34] Overall, the low toxicity of the reagents used, combined with the simplicity and the scalability of the synthetic pathway described in Figure 1c, makes this process attractive for the production of these materials on an industrial scale.

The UV–vis absorption spectrum of **P4a** in toluene solution is shown in Figure 1b (**P4b** and P4c present similar characteristics, see also the Supporting Information, Fig. S1). As expected, in analogy with **P1**–**P3**, **P4a** exhibits a dual band of absorption, in this case peaking at 368 and 662 nm, respectively, in turn leaving a well of transmission extended over the entire blue region (420–490 nm) of the visible light, with a local minimum of absorption at 432 nm. Importantly, **P4a**–**P4c** show only minor optical changes upon elevating the temperature (ambient to 100 °C), indicating neither significant disruption of effective conjugation nor major aggregation of the solvated backbones.

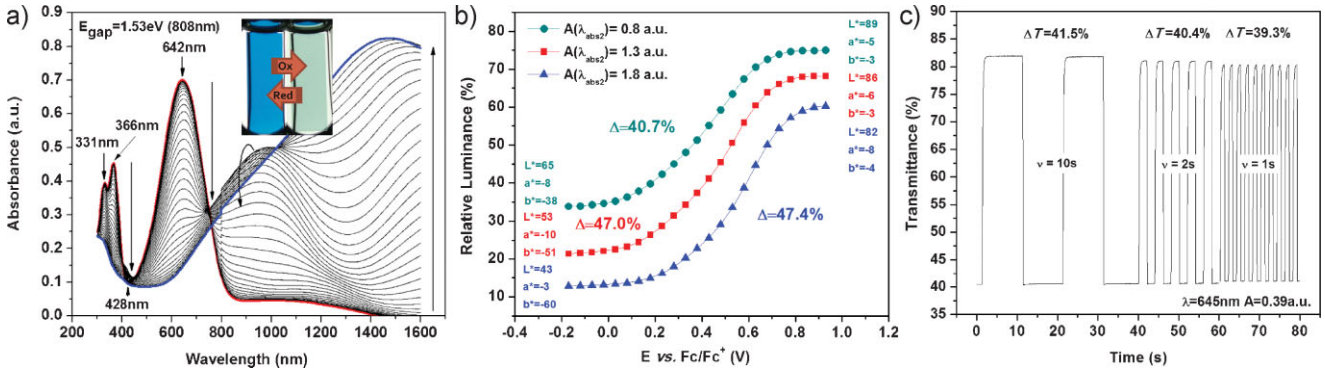

Figure 2. a) Spectroelectrochemistry of **P4b**. The films were spray-cast onto ITO-coated glass from a mixture of toluene and chloroform (1 mg mL^{-1}). Electrochemical oxidation of the films was carried out in 0.1 M $LiBF_4$/PC supporting electrolyte using a silver wire as a quasireference electrode (calibrated against Fc/Fc$^+$) and a platinum wire as the counter electrode. The applied potential was increased in 25 mV steps from 0 to 0.95 V vs. Fc/Fc$^+$. b) Relative luminance (%) as a function of applied potential for spray-coated **P4b**. For color matching, $L^*a^*b^*$ values of fully neutral and oxidized states are reported for the films. c) Squarewave potential-step absorptiometry of **P4b** (monitored at 642 nm, −0.4 to +0.96 V vs. Fc/Fc$^+$ in 0.2 M Li BTI/PC solution electrolyte). The switch time was 10 s step for 40 s (2 cycles), then 2 s step for 20 s (5 cycles), and 1 s step for 20 s (10 cycles).

Thin films of **P4a** and **P4b** were spray-cast onto indium tin oxide (ITO)-coated glass slides from warm mixtures of toluene and chloroform (ca. 40 °C) and, subsequently, redox cycled until a stable and reproducible switch was obtained prior to spectroelectrochemical analysis. **P4a** and **P4b** were found to possess relatively narrow bandgaps of 1.51 eV, and 1.53 eV respectively, as determined from the onset of their neutral-state lower-energy optical transition. An external bias was applied to the polymer films placed in a three-electrode electrochemical cell and was gradually increased (in 25 mV steps) to induce simultaneous bleaching (starting at ca. 0.12 V vs. Fc/Fc$^+$) of both the short- and long-wavelength absorption bands in the UV–vis region. The depletion of the neutral-state optical absorption of the copolymers was accompanied by the concomitant formation of new transitions arising in the near-IR region of the spectrum (see Fig. 2a), indicating the development of radical cations (polarons), further combining into dications (bipolarons) at higher biases. Interestingly, the linearly substituted copolymer **P4b** switched more effectively to its transmissive oxidized state on full doping in comparison with the nearly identical, yet branch-substituted analogue **P4a** (see Supporting Information, S2). This can practically be seen from the extent of overlap of their respective bipolaronic optical transition with the visible spectrum (in the 600–800 nm range). Here, the bipolaronic transition of **P4a** peaks at wavelengths lower than 1400 nm, while that of **P4b** peaks above 1400 nm (at ca. 1460 nm), as can be seen from Figure 2a, and tails less into the visible. It is worth noting that the opposite trend has frequently been observed in π-conjugated polymers with various substitution patterns, as the best candidates tend to be the ones likely to exhibit the most open morphologies, in correlation with their ability to facilitate the diffusion of charge-balancing ions occurring on redox doping/dedoping.[4,6,10,35–37] The better ''packing ability'' of the linearly substituted derivative **P4a** on full oxidation may explain the notable bathochromic shift undergone by its bipolaronic transition in the near-IR. In parallel, thin films of **P4b** start oxidizing at slightly lower potentials (+0.05 V vs. Fc/Fc$^+$) than those of **P4a** (+0.12 V vs. Fc/Fc$^+$), as supported by differential pulse voltammetry (see S3), whereby the onset of oxidation of **P4b** occurs at slightly less positive potentials (ca. −0.16 V) than that of **P4a** (ca. +0.09 V). The resulting higher HOMO level of **P4b** may further contribute to its propensity to produce more transmissive oxidized states upon electrochemical doping. Based on those spectroelectrochemical data, **P4a** exhibits an EC contrast (i.e., a monochromatic change in transmittance, Δ%T) in the order of 40% at its longer-wavelength absorption maximum (663 nm), while values as high as 52% were attained with **P4b** at the same long-wavelength absorption maximum (642 nm).

Monitoring the brightness of transmitted light as a percentage of the brightness of a light source calibrated to the sensitivity of the human eye, the relative luminance change was measured for the films upon increasing the doping level induced by electrochemical oxidation. Here, **P4a** was found to switch from its neutral state, blue, to its highly transmissive oxidized state with up to 44% change in relative luminance (see S4), while films of **P4b** of near-equal thickness, and even thicker, exhibited up to ca. 47%, as illustrated in Figure 2b. The saturated blue color of the neutral-state polymers was supported by a colorimetry study, which indicated largely negative b^* values at all film thicknesses, along with especially small a^* values (negative values indicating the extent of green hue) in comparison with b^* ($L^*a^*b^*$ refers to the Commission internationale de l'éclairage (CIE) 1976 $L^*a^*b^*$ color model). Upon full oxidation, **P4b** exhibits L^* values ranging from 82 to 89 depending on the optical density of the deposited film. Further, with a^* and b^* values as low as −5 and −3, respectively, **P4b** yields transmissive states in which residual tints can hardly be perceived by the human eye, demonstrating the aptitude of the electrochrome to nearly reach the ''white point'' of color space. In comparison, higher-optical-density films of **P4a** do not show the same propensity to bleach and a trade-off in terms of contrasts observed can be found for films with optical densities greater than 1.1 a.u. This reduction in electrochromic contrast with increased thickness observed in the case of **P4a** has been previously observed in other polymer electrochromes.[35] Overall, the polymers complete their full switches in a potential window of less than 1 V (90% of optical change is attained in ca. 0.5 V for **P4a** and ca. 0.8 V for **P4b**), a parameter of significant interest for low-voltage device applications.

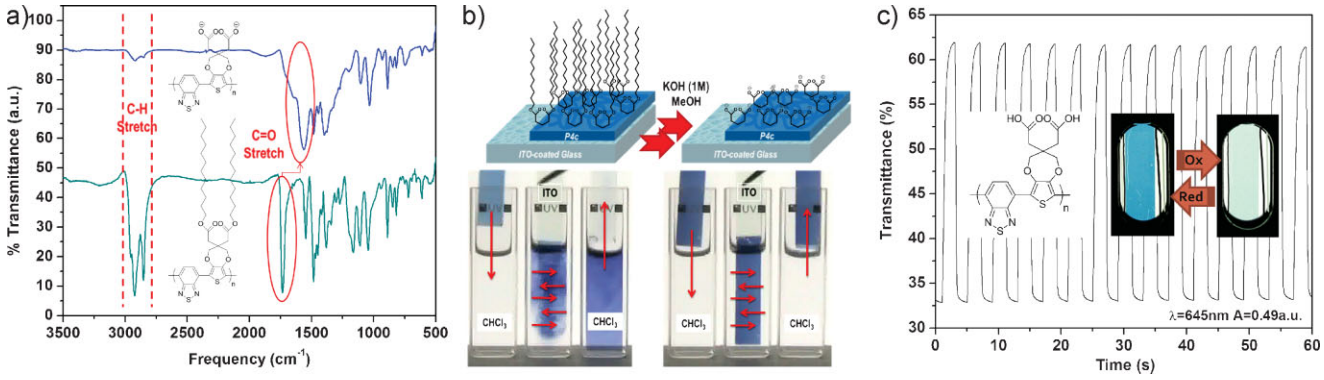

Figure 3. a) IR absorption spectra of **P4c** before (bottom) and after (top) defunctionalization of the solubilizing side chains. The spectrum before defunctionalization was taken from a thin film of **P4c** deposited on a NaCl plate, defunctionalized **P4c** was taken from a pressed KBr pellet. b) Illustration of the difference in solubility observed before and after saponification of the thin films. Non-defunctionalized films dissolve instantaneously on immersion in $CHCl_3$ (left set of photographs) in contrast to the saponified ones (right set of photographs). c) Squarewave potential-step absorptiometry of **P4c** monitored at 645 nm, −0.56 to +0.80 V vs. Fc/Fc^+ in 0.2 M Li BTI/PC solution electrolyte. The switch time was 2 s step for 60 s (15 cycles).

The EC contrasts for the polymers ($\Delta\%T$) were monitored as a function of time at their longer-wavelength absorption maximum by applying squarewave potential steps of 10, 2, and 1 s. In this case, the 0.1 M $LiBF_4$/PC solution electrolyte system used throughout the spectroelectrochemical and colorimetric experiments was replaced by a 0.2 M lithium bis(trifluoromethanesulfonyl)imide (LiBTI)/PC solution electrolyte, which was found to significantly improve the response times for the polymers (while time was not a factor of importance in the previous experiments). As illustrated in Figure 2c, a variation of EC contrast ($\Delta\%T$) of only ca. 2% was monitored in the case of **P4b** on decreasing the switch time from 10 s to 1 s, an important result when considering the execution speed in switchable display devices. Further, in agreement with the spectroelectrochemical data, the EC contrast attainable with **P4b** (e.g., 41.5% when $\nu = 10$ s) on repeated squarewave potential stepping was found higher than that of **P4a** (e.g., 35.2% when $\nu = 10$ s) for films of near-identical optical density. While **P4b** was found to reach its full switch faster than **P4a**, both polymers attained 95% of a complete switch in less than 1 s ($t_{95\%} = 0.80$ s in the case of **P4a**, $t_{95\%} = 0.45$ s in the case of **P4b**), again, reinforcing their potential for applications in products such as displays, which require fast response times.

The long-term stability of the polymers was investigated by monitoring the EC contrast ($\Delta\%T$) of the thin films (as described in Fig. 2c) upon repeated squarewave potential steps of 1 s (complete cycle is 2 s) in a 0.2 M LiBTI/PC solution electrolyte system. In over 10000 cycles under ambient conditions, **P4a** and **P4b** showed a variation of EC contrast ($\Delta\%T$) of less than 7% (see Fig. S5), hence, satisfying the requirements for polymer electrochromes applicable to cost-effective ambient device-manufacturing processes.

Encouraged by the excellent results obtained with **P4a** and **P4b** in terms of contrast, response times, and switching stability, we developed the didodecylester-substituted DA copolymer analogue **P4c** with the perspective of cleaving its solubilizing side chains via a basic hydrolysis of the esters (saponification) achieved directly from the thin films. Conjugated polymers that can be solution-processed and, subsequently, defunctionalized to produce films insoluble in most conventional organic solvents have recently emerged for use in EC and multilayer light-emitting diode (LED) devices,[38] transistors,[39] and photovoltaic cells.[40] In the case of **P4c**, we found that the spray-cast polymer can be effectively defunctionalized by immersing the films in a 1 M KOH methanol solution for 4 h at 70 °C. As demonstrated in Figure 3a, the same conditions can be applied to the saponification of the finely ground polymer itself, hence, replacing the aliphatic esters by carboxylate functionalities on each ProDOT heterocycle along the backbone. Here, the conversion from the esters to the carboxylates is evidenced by a distinct shift of the C=O stretching band towards lower frequencies (from 1734 to 1560 cm^{-1}), along with a broadening of the corresponding band. In parallel, the loss of the aliphatic side chains is clearly visible through the depletion of the C−H-stretching-band intensity at higher frequencies (2800–3000 cm^{-1}). Figure 3b illustrates the differences in solubility for the DA polymer before and after saponification, with the non-defunctionalized film dissolving instantaneously on immersion in $CHCl_3$ (left set of photographs), while the saponified counterpart holds to the substrate (right set of photographs), even after prolonged exposure to the solvent or on elevation of the temperature. As seen in Figure 3c, a series of squarewave potential steps applied to a defunctionalized thin film of **P4c** confirms that the electroactivity of the electrochrome is retained throughout the defunctionalization process. Here, the freshly hydrolyzed film was rapidly neutralized in an aqueous solution of HCl (1 M) and subsequently rinsed with methanol, prior to electrochemical switching. Further work exploring the performance and the solubility of this structurally modified ECP is underway, including the construction of display devices with architectures taking advantage of the solubility change undergone by the electrochrome.

In summary, a series of spray-processable π-conjugated polymer electrochromes switching from a saturated-blue to a highly transmissive oxidized state on electrochemical doping were designed with strictly alternating electron-rich and -poor heterocycles, and synthesized by Suzuki polycondensation. In this study, the dual band of absorption often found in DA macromolecular π-conjugated systems[15,19–22] was modulated by reducing the extent of electron-rich units along the polymer

ADVANCED MATERIALS
www.advmat.de

www.MaterialsViews.com

backbone to a point where the short-wavelength absorption band of the polymer is fully transferred into the UV, hence, opening a broad window of transmission in the blue region of the visible spectrum. In contrast, more electron-rich parent copolymers have been found to possess a two-band absorption in the visible, in turn exhibiting colors ranging from blue-green to green.[15,16] Optical and electrochemical investigation of the neutral-state blue electrochromes revealed excellent optical contrasts, both in the visible and in the near-IR, small potential windows of operation, fast switching times, and long-term stability. Besides the initial solution-processability of all the polymer precursors described in this Communication, the postdeposition saponification of thin films of ProDOT–BTD copolymer electrochromes substituted with alkyl ester side-chains offers unique perspectives for the construction of long-lived electrolyte-based display devices, as well as in the processing of vertically-stacked ECDs with multiple electroactive layers.

Acknowledgements

We gratefully acknowledge funding of this work by the AFOSR (FA9550-09-1-0320) and thank Svetlana Vasilyeva for assistance with electrochemical measurements, and Sam Popwell for gPC measurements. Supporting Information is available online from Wiley InterScience or from the author.

Received: August 24, 2009
Published online: December 15, 2009

[1] P. M. S. Monk, R. J. Mortimer, D. R. Rosseinsky, *Electrochromism and Electrochromic Devices*, Cambridge University Press, New York **2007**.
[2] F. C. Krebs, *Nat. Mater.* **2008**, *7*, 766.
[3] G. Dennler, M. C. Scharber, C. J. Brabec, *Adv. Mater.* **2009**, *21*, 1323.
[4] B. Sankaran, J. R. Reynolds, *Macromolecules* **1997**, *30*, 2582.
[5] A. Kumar, J. R. Reynolds, *Macromolecules* **1996**, *29*, 7629.
[6] A. Kumar, D. M. Welsh, M. C. Morvant, F. Piroux, K. A. Abboud, J. R. Reynolds, *Chem. Mater.* **1998**, *10*, 896.
[7] H. W. Heuer, R. Wehrmann, S. Kirchmeyer, *Adv. Funct. Mater.* **2002**, *12*, 89.
[8] C.-G. Wu, M. I. Lu, S. J. Chang, C. S. Wei, *Adv. Funct. Mater.* **2007**, *17*, 1063.
[9] M. A. Invernale, V. Seshadri, D. M. D. Mamangun, Y. Ding, J. Filloramo, G. A. Sotzing, *Chem. Mater.* **2009**, *21*, 3332.
[10] M. Li, Y. Sheynin, A. Patra, M. Bendikov, *Chem. Mater.* **2009**, *21*, 2482.
[11] B. D. Reeves, C. R. G. Grenier, A. A. Argun, A. Cirpan, T. D. McCarley, J. R. Reynolds, *Macromolecules* **2004**, *37*, 7559.
[12] E. E. Havinga, W. Hoeve, H. Wynberg, *Synth. Met.* **1993**, *55*, 299.
[13] B. C. Thompson, Y. G. Kim, T. D. McCarley, J. R. Reynolds, *J. Am. Chem. Soc.* **2006**, *128*, 12714.
[14] A. Balan, G. Gunbas, A. Durmus, L. Toppare, *Chem. Mater.* **2008**, *20*, 7510.
[15] P. M. Beaujuge, S. Ellinger, J. R. Reynolds, *Nat. Mater.* **2008**, *7*, 795.
[16] P. M. Beaujuge, S. Ellinger, J. R. Reynolds, *Adv. Mater.* **2008**, *20*, 2772.
[17] G. Sonmez, C. K. F. Shen, Y. Rubin, F. Wudl, *Angew. Chem. Int. Ed.* **2004**, *43*, 1498.
[18] G. Sonmez, H. B. Sonmez, C. K. F. Shen, R. W. Jost, Y. Rubin, F. Wudl, *Macromolecules* **2005**, *38*, 669.
[19] N. Blouin, A. Michaud, D. Gendron, S. Wakim, E. Blair, R. Neagu-Plesu, M. Belletete, G. Durocher, Y. Tao, M. Leclerc, *J. Am. Chem. Soc.* **2008**, *130*, 732.
[20] E. Bundgaard, F. C. Krebs, *Macromolecules* **2006**, *39*, 2823.
[21] A. Durmus, G. E. Gunbas, P. Camurlu, L. Toppare, *Chem. Commun.* **2007**, 3246.
[22] D. Mühlbacher, M. Scharber, M. Morana, Z. Zhu, D. Waller, R. Gaudiana, C. Brabec, *Adv. Mater.* **2006**, *18*, 2884.
[23] A. P. Kulkarni, Y. Zhu, A. Babel, P.-T. Wu, S. A. Jenekhe, *Chem. Mater.* **2008**, *20*, 4212.
[24] S. A. Jenekhe, L. Lu, M. M. Alam, *Macromolecules* **2001**, *34*, 7315.
[25] U. Salzner, *J. Phys. Chem. B* **2002**, *106*, 9214.
[26] U. Salzner, M. E. Kose, *J. Phys. Chem. B* **2002**, *106*, 9221.
[27] O. Karalt, S. Durdağı, U. Salzner, *J. Mol. Model.* **2006**, *12*, 687.
[28] Z. Zhu, D. Waller, R. Gaudiana, M. Morana, D. Muhlbacher, M. Scharber, C. Brabec, *Macromolecules* **2007**, *40*, 1981.
[29] R. Yang, A. Garcia, D. Korystov, A. Mikhailovsky, G. C. Bazan, T.-Q. Nguyen, *J. Am. Chem. Soc.* **2006**, *128*, 16532.
[30] W. Yue, Y. Zhao, S. Shao, H. Tian, Z. Xie, Y. Geng, F. Wang, *J. Mater. Chem.* **2009**, *19*, 2199.
[31] J. Hou, H.-Y. Chen, S. Zhang, G. Li, Y. Yang, *J. Am. Chem. Soc.* **2008**, *130*, 16144.
[32] M. Zhang, H. N. Tsao, W. Pisula, C. Yang, A. K. Mishra, K. Mullen, *J. Am. Chem. Soc.* **2007**, *129*, 3472.
[33] T. Hoi Nok, C. Don, A. Jens Wenzel, R. Ali, W. B. Dag, P. Wojciech, K. Mullen, *Adv. Mater.* **2009**, *21*, 209.
[34] R. N. Brookins, K. S. Schanze, J. R. Reynolds, *Macromolecules* **2007**, *40*, 3524.
[35] P. M. Beaujuge, S. V. Vasilyeva, S. Ellinger, T. D. McCarley, J. R. Reynolds, *Macromolecules* **2009**, *42*, 3694.
[36] G. A. Sotzing, J. R. Reynolds, P. J. Steel, *Chem. Mater.* **1996**, *8*, 882.
[37] C. L. Gaupp, D. M. Welsh, J. R. Reynolds, *Macromol. Rapid Commun.* **2002**, *23*, 885.
[38] B. D. Reeves, E. Unur, N. Ananthakrishnan, J. R. Reynolds, *Macromolecules* **2007**, *40*, 5344.
[39] A. R. Murphy, J. M. J. Frechet, P. Chang, J. Lee, V. Subramanian, *J. Am. Chem. Soc.* **2004**, *126*, 1596.
[40] J. Liu, E. N. Kadnikova, Y. Liu, M. D. McGehee, J. M. J. Frechet, *J. Am. Chem. Soc.* **2004**, *126*, 9486.
[41] K. Pilgram, M. Zupan, R. Skiles, *J. Heterocycl. Chem.* **1970**, *7*, 629.